Design of a Rugged Wheel for Application in the Leveraged Freedom Chair

by

Sara Elizabeth Falcone

Submitted to the
Department of Mechanical Engineering
in Partial Fulfillment of the Requirements for the Degree of

Bachelor of Science

at the

Massachusetts Institute of Technology

June 2015

Signature of Author: Signature redacted
Department of Mechanical Engineering
May 8, 2015

Certified by: Signature redacted
Daniel Frey
Professor of Mechanical Engineering
Thesis Supervisor

Accepted by: Signature redacted
Anette Hosoi
Professor of Mechanical Engineering
Undergraduate Officer

Design of a Rugged Wheel
for Application in the Leveraged Freedom Chair

by

Sara Elizabeth Falcone

Submitted to the
Department of Mechanical Engineering on May 8, 2015
in Partial Fulfillment of the Requirements for the Degree of Bachelor of Science in Mechanical Engineering

Abstract

This thesis analyses the front wheel of the Leveraged Freedom Chair (LFC) an all-terrain, off-road wheelchair with two distinct models: one for the developing world and one specifically for American riders. The functional requirements of performance and price, were designated by the start-up company Global Research Innovation and Technology (GRIT), which makes the LFC.

This study includes comparisons between the original rubber wheel, which is currently being used as the front wheel of the LFC, and alternative wheels available for purchase. The goal was to find a new wheel which could be implemented for future manufacturing to increase the lifespan of the LFC, improve the ride quality and efficiency of production.

Based on performance it is concluded that a pneumatic wheel of comparable geometry to the original rubber wheel is the best alternative for the American chair where maintenance is more routine and replacement parts and service are readily available. For the developing world future work is necessary to either improve the quality of the original rubber wheel or select a low cost, low maintenance alternative.

Thesis Supervisor: Daniel Frey

Title: Professor of Mechanical Engineering

Acknowledgments

I would like to thank many people, including my friends and family, for their help and guidance throughout my time as an MIT Undergraduate. Specifically I would like to acknowledge Mr. Mario Bollini of the Global Research Innovation and Technology team for his inspiration, guidance through India and encouragement to work on the Leveraged Freedom Chair. Much appreciation goes to Professor Dan Frey for his advice and enlightenment throughout the writing and design process.

Contents

List of Figures

List of Tables

1. Introduction

1.1 Motivation

The Leveraged Freedom Chair (LFC) is an off road wheel chair designed to overcome obstacles, such as sloped terrain and bumps, more easily than a standard hospital chair. The cantilevered front caster wheel moves the center of gravity forward, allowing rider to tip further back while still maintaining stability. The levers and drive train allow the rider to "gear" putting their hands higher up for more torque and lower down when they wish to achieve more velocity, which can be seen in Figure 1.

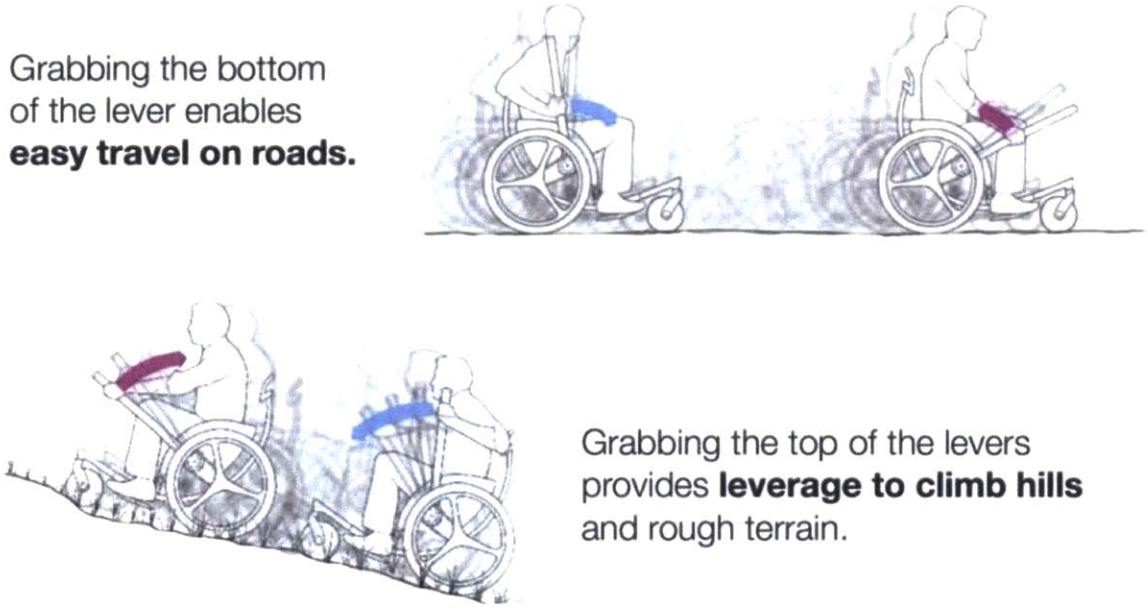

Figure 1: The novel "gearing" mechanism of the LFC [3].

The LFC is made by a start –up called Global Research Innovation and Technology (GRIT) which came out of MIT. There are two distinct versions of the LFC, both depicted in Figure 2. On the left is the design for developing countries and on the right the model specifically for American clients. The developing world LFC is slightly simpler in design and more affordable than the American version, which has a higher standard of components, and is slightly larger as it is specifically design for a demographic of westerners and sports wheel chair enthusiasts.

Both versions of the LFC are currently produced with the same rubber wheel, which has reportedly failed within a year of use due to the rubber cracking and misalignments inducing a speed wobble. As this wheel is not meeting the functional requirements of the GRIT Team an alternative wheel is being sought.

Figure 2: Developing world LFC on the left and the American LFC on the right [3].

1.2 Current Front Wheel Design and Problems

The front wheel of the LFC is a rotating caster wheel with a negative caster angle, keeping the steering axis under the rider, allowing them to turn as they would in a standard wheel chair. Figure 3 labels the characteristics of a caster wheel with its commonly used terminology.

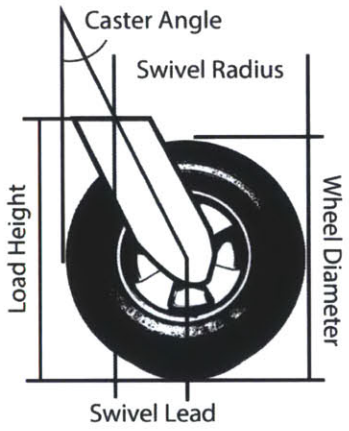

Figure 3: Diagram labeling caster wheel geometry.

The front wheel assembly drops below the front of the boom, as pictured in Figure 2. The connection is made with a bicycle headset on the American chair and a bottom bracket on the developing world chair. These bearing mechanisms connect to a fork made of a pressed steel plate on the American chair and welded CNC bent pipes on the developing world LFC. A solid model of the front wheel assembly for the American LFC is shown in Figure 4. "The fork geometry (caster angle, trail) was adopted from the Worldmade chair, as was the molded rubber caster wheel" [1, 7].

Figure 4: American LFC Front Wheel Assembly.

Throughout this paper the term wheel is used to describe the entire rolling mechanism, including both the tire and the hub, shown in Figure 5. The hub is the part of the wheel connecting the tire to the axle, including the bearings. The tem "tire" describes the elastic ring surrounding the hub.

Figure 5: Visual representation of wheel, tire, hub terminology.

Both versions of the LFC are designed to use the same front wheel, which is a molded rubber caster wheel. As the chair has no suspension it is predicted that the elasticity or springiness of the wheels absorbs much of the shock when riding over bumps, increasing user comfort over stiff wheels. The rear wheels of the chair are standard 26" pneumatic bicycle wheels and the front wheel is currently a solid piece of molded rubber. Inspecting chairs which have been ridden for approximately 7 months, a few have experienced cracking of the rubber, particularly between the front holes, though in the sample depicted in Figure 6 cracking is also visible along the rims edge. Due to these failures a pre-manufactured replacement for the front wheel is being sought.

Figure 6: Visible cracks in the rubber of original front wheels which had been ridden for less than a year.

The current front wheel is a solid piece of compression molded natural rubber with a central hole left to insert a hub. It is made out of natural rubber manufactured at Super Rubber Industries in Indore, India. The rubber is vulcanized with one 30 minute cycle at 150°C, controlling the temperature and time. Approximately 0.01% sulfur is added, in addition to "antioxidants, accelerators, curing agents, wax, carbon black, rubber process oil, resins etc." [12]. Through several iterations of molding shots, the final wheel geometry is formed. In the last iteration, rubber sheets are placed and wrapped around the edges of the wheels mold, encasing the molded rubber shot, which is approximately the wheels' geometry. The rubber is heated again to laminate the sheets and the shot. The mold is taken out of the heat press and the wheel is removed for cooling.

A bicycle front hub purchased from the local market in Indore, India is then hammered into the central hole of the wheel. The rubber deforms a significant amount allowing the hub to pop through and seat within the wheel, which relaxes back to its natural geometry. The hub assembly is depicted in Figure 7. The bearings are hand packed and two cones are added on either side, hand tightened and sandwiched in place by two lock nuts on each side. The axle is a threaded rod, which seats into the fork and it held in place by two more nuts.

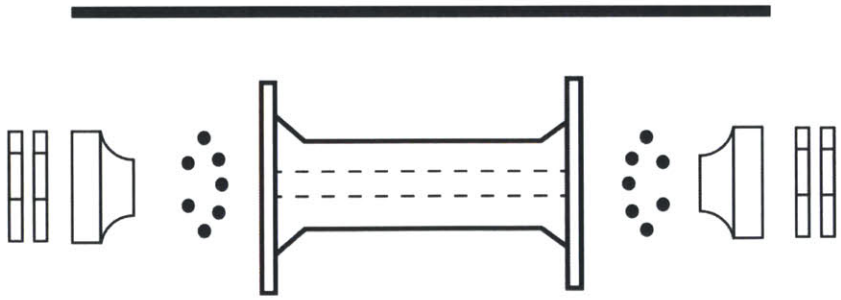

Figure 7: Diagram of the hub, bearings, bearing cone, double lock nuts and axle.

Limitation in the manufacturing facility and process prevent the implementation of a control point which could guarantee the alignment of the hub within the wheel, excluding a visual inspection. The flanges on the sides of the hub hopefully ensure its alignment, but not to any precision. This leads to the suspicion

that the tire and the wheel are not square to each other, as demonstrated by Figure 8, showing an elevation view of a misaligned wheel as it rotates forward 90 degrees. This misalignment would bring cyclic loading perpendicular to the face of the wheel as it rotates, causing tension and compression to bend the wheel sideways. This could plastically deform the areas around the hole, which boast the highest stress concentration factors, and may be leading to the material failures seen in the wheel as shown in Figure 6. This missalignment, or another similar, is also suspected to cause the "speed wobble" where the wheel wobbles, or zig-zags, as the chair rides along a straight path. This is uncomfortable for the rider and prevents affected LFCs from reaching their maximum potential speed.

Figure 8: Visual of hub misalignment causing the tire and wheel to not be square.

2. Design Criteria

2.1 Functional Requirements

Discussions with the GRIT team resulted in the following functional requirements [6] for the front wheel of the Developing World LFC. All of the listed functional requirements were consulted and considered throughout the design process.

1. Life span of 10 years
    a. Withstand forces and wear associated with daily chair use in rugged conditions
    b. Puncture resistant or easy to find replacement tubes
2. Light weight
    a. Lighter than current front wheels weight of 1.735kg
    b. ~8.75" diameter
3. An appropriate amount of elastic compliance to maximize rider comfort
4. Able to float over loose gravel/soil rather than digging in. the current wheel has a wide footprint making it easier to roll over soft ground.
5. Low cost
    a. Less than, or equal to, $12 per wheel, which is the price of the current rubber wheel

2.2 Forces

To determine the force for which to design, previous work by Benjamin Judge was consulted and his assumptions were held throughout this experiment and paper. "For expected loading on the model wheelchair, a 225lb mass (an approximated person) was equally distributed between the front and two rear rigid points of contact between the seat and the frame. Additionally, a conservative design factor of two takes into account potential impact forces and member fatigue over time. This equates to a maximum design load of 2000N" [10].

Balancing forces in the vertical plane as shown in Equation 1, and balancing the moment about the back wheels, F_{BW}, in Equation 2 the static load on the front wheel, F_{FW}, is equated in Equation 3 as a function of the length of the boom, L, and the distance the center of gravity is in front of the back wheels, X.

$$-2000[\mathrm{N}] + F_{\mathrm{FW}} + 2 \cdot \mathrm{F_{BW}} = 0 \tag{1}$$

$$F_{\mathrm{FW}} \cdot X - 2000[N](L - X) = 0 \tag{2}$$

$$F_{\mathrm{FW}} = \frac{2000[\mathrm{N}](\mathrm{L}-\mathrm{X})}{\mathrm{L}} \tag{3}$$

These calculations show that if the T frame is 1.5m long, and the seat is centered 0.1m in front of the rear wheels axles, the force on the front wheel is 1,870N.

To model the loading of the front wheel as it is passes over a bump work by John Michael Walton was consulted which relates the height of an obstacle and the torque necessary for the rider to apply to the

levers to overcome it in a static situation [9]. Figure 9 is a diagram labeling the forces on the chair and characteristic elements of the geometry.

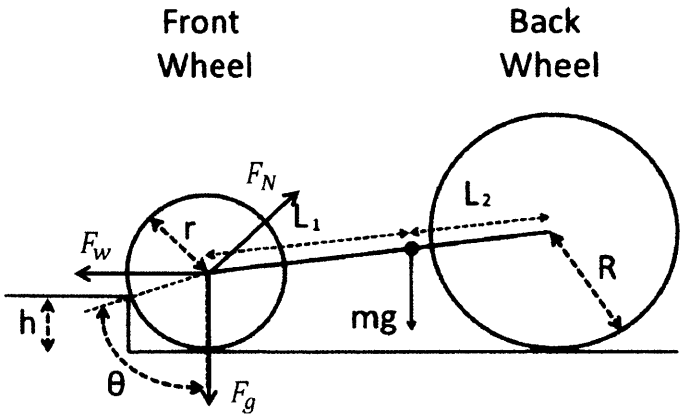

Figure 9: Performance analysis setup and free body diagram for the LFC climbing and obstacle [9].

Balancing of forces in Figure 9, force from gravity F_g, normal force F_N, and the force that the riders applied torque provides to the front tire F_W, as described on page 15 of Walton's thesis, yields Equation 4 relating the torque, T, necessary for the rider to apply to the lever with the chair's geometry and the height of the obstacle.

$$T = \frac{mgR}{(1+\frac{L_1}{L_2})(\frac{r-h}{r})} \tag{4}$$

2.3 Materials Background

Common materials from which wheels are molded include polyurethane foam, vulcanized rubber and a pneumatic rubber tire-tube combination. Polyurethane foam is "a highly nonlinear material, not isotropic, and changes in its density dramatically effect its stress-strain response" [2]. Rubber is a well-studied, highly used elastic material. It is found that below a critical severity of strain no crack propagation will occur, in the absence of chemical corrosion. This severity defines a fatigue limit for repeated stressing, below which the life of the rubber can be virtually indefinite [11]. All of these materials exhibit viscoelastic properties, as when they are deformed each returns to its original geometry but is also rate dependent.

These materials can be mechanically modeled as a system of springs and dashpots to assimilate their response to forces and loading. Here the front wheel is modeled as a Kelvin-Voigt viscoelastic material by considering the entire wheel as a single spring and dashpot in parallel, shown in Figure 10. Springs describe the amount the material forces back from a deformation, modeling the materials elastic behavior, and a dashpot shows the amount of energy absorbed by the deformation, modeling its viscous characteristics [4].

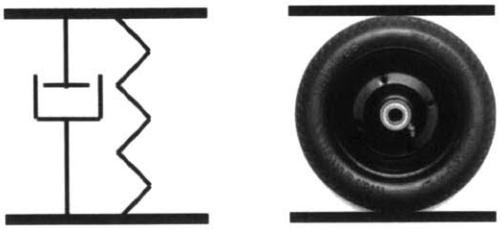

Figure 10: Kelvin-Voigt model of the wheel as a single spring and dashpot in parallel.

Material elasticity is typically compared via each materials characteristic elastic modulus, or Young's modulus, E, as a function of stress, σ, and strain, ε, shown in Equation 5 [8].

$$\sigma = \mathrm{E} \cdot \varepsilon \tag{5}$$

However, in this experiment the displacement of the top of the wheel, x, as the wheel is compressed from the neutral position is measured as the result of an applied force. Because the wheel deforms as a load is applied, its contact surface area with the force plate varies, and thus determining the wheels stress requires an additional measurement to determine the changing contact area. To reduce inconsistencies which would occur from an inaccurate contact surface area estimation the following comparisons are left in terms of force versus displacement. The front wheel is here modeled as a single spring. Using Hooke's law, Equation 6, the spring constant, k, of each wheel is determined and used to compare their stiffness.

$$\mathrm{F} = -\mathrm{k} \cdot \mathrm{x} \tag{6}$$

Hysteresis is a term used to describe a time dependency of a system. Specifically, elastic hysteresis describes the energy dissipated within an elastic material due to internal friction over a compressive and decompressive cycle [4]. Analyzing the units of integrating the area within a stress-strain curve shows force times extension, giving N·m, or Joules, the unit of energy.

Modeling the front wheel as a spring and a dashpot we can incorporate the area within the hysteresis loop as a damping coefficient, b, with the use of Equation 7 relating the force on a dashpot, F, and the velocity at which it is contracting, $\dot{\mathrm{x}}$.

$$F(t) = b \cdot \dot{\mathrm{x}} \tag{7}$$

Incorporating the relationship of Equation 7 with Equation 8 [13], which uses description of energy as the integral of force by distance, an relationship for the energy dissipated within a dashpot, E, can be derived as a function of its velocity, $\dot{\mathrm{x}}$, and a characteristic damping coefficient, b.

$$E = \int_0^x f(x) \cdot dx = \int_0^t F(t) \cdot \frac{dx}{dt} \cdot dt = b \int_0^t \dot{x}(t)^2 \cdot dt \tag{8}$$

As an ideal spring does not absorb energy, in this model where the wheel is represented solely by a spring and dashpot in parallel, all energy absorbed into the wheel is taken up by the dashpot. Therefore the area measured within the hysteresis loop can be equated to Equation 8, resulting in a numerical value for the damping coefficient of each wheel, b.

3. Wheel Measurements and Experimentation

3.1 Original Front Wheel Acceleration Experiment

To determine the active forces experienced by the front wheel an accelerometer was used to measure the 3-axis acceleration while riding the chair. The accelerometer was attached to the boom directly above the front wheel as shown in Figure 11. The chair was ridden over smooth surfaces, a rough sidewalk and the front wheel dropped from known heights up to 10 inches off the ground, while the two rear wheel remained level on the ground. The rough sidewalk was a stretch of broken up cement netted with rocks and cracks many centimeters in depth and width.

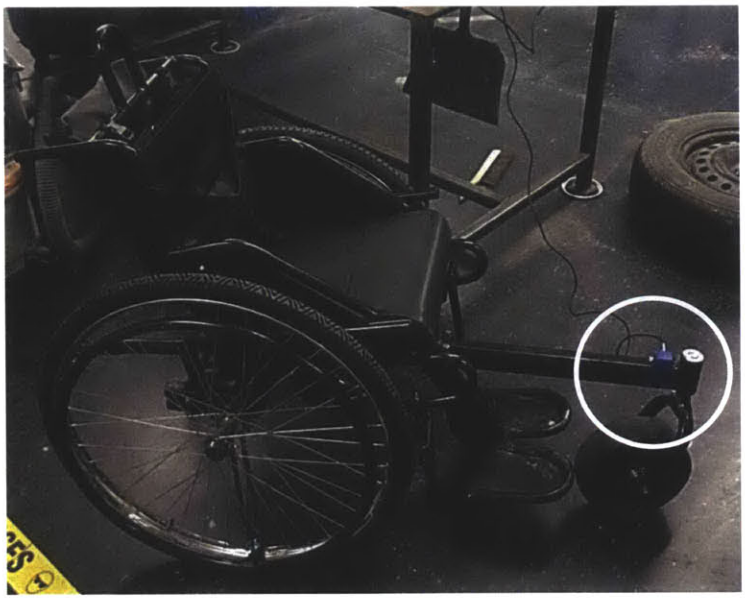

Figure 11: Accelerometer adhered to the front of the boom directly above the front wheel of the LFC.

Figure 12 depicts the 3 directional acceleration data collected while riding over "bumpy terrain." The peak acceleration of 42.9 $\frac{m}{s^2}$ is called out to give an idea of the forces experienced by the wheel. In a conservative calculation it is believable the chair could see a force of 5,000N. In Section 2.2 the rider was said to weigh 225lb or about 100kg. If the entire weight of the rider and the chair were supported solely by the front wheel, which could be the case if the chair fell off a curb or hit a large bump, accelerations of $50\frac{m}{s^2}$ would yield forces of 5,000N. In Section 3.2 a 5,000N force is seen to crack the original wheel immediately in the Instron testing. This is affirmation that the original front wheel cannot meet the functional requirements of the GRIT team for the LFC and needs to be replaced with a higher quality, stronger alternative for both the developing world and American chair.

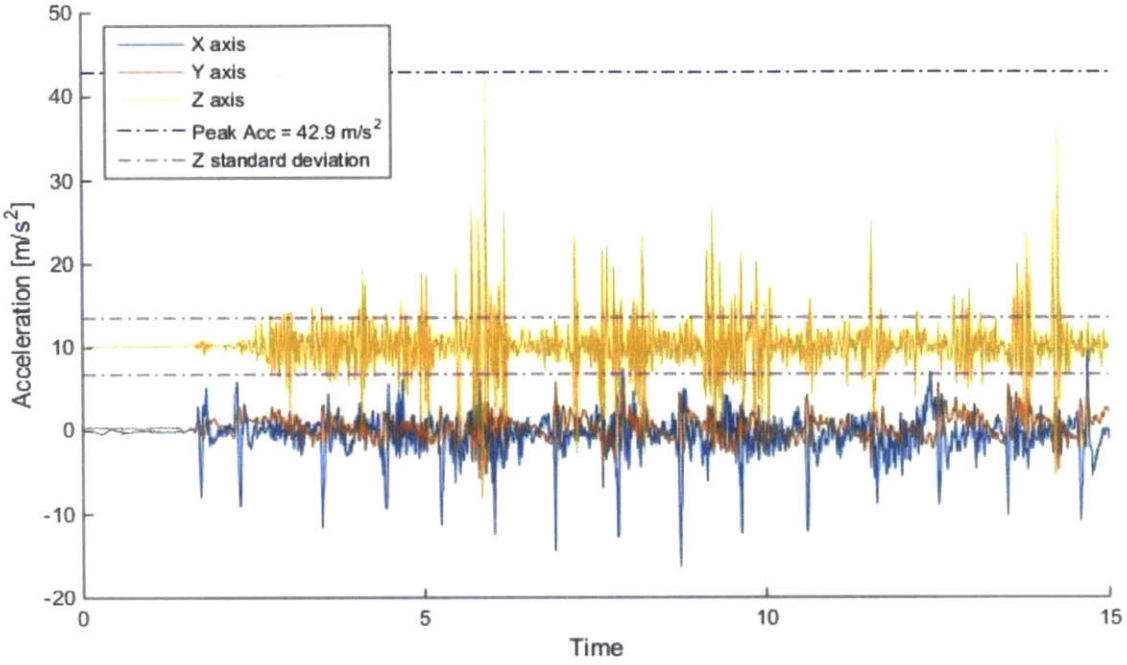

Figure 12: Measured acceleration on the boom above the front wheel while riding over bumpy terrain.

A Fast Fourier transform of the z-axis acceleration measured signal from Figure 12 is shown in Figure 13. The sharp central peak with no second peak shows that the z-axis acceleration over this bumpy surface does not follow a cyclic pattern. This is not surprising as the roughness of the terrain was not of a cyclic nature.

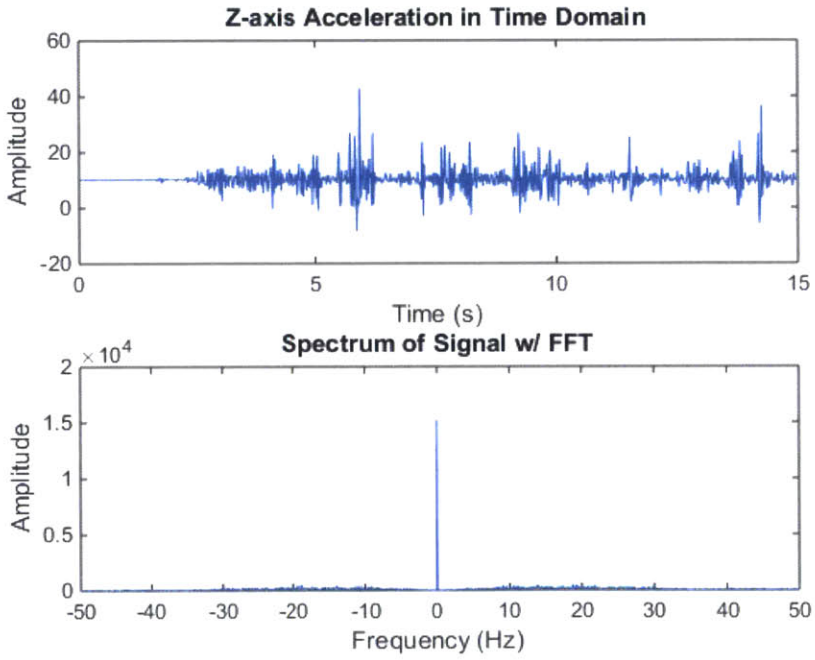

Figure 13: Comparison of the Z-axis acceleration data for bumpy terrain in the time and frequency domains.

In comparison a Fast Fourier transform of the x-axis acceleration measured signal from Figure 12 is shown in Figure 14. This acceleration is expected to follow a cyclic pattern as the rider pumps the levers of the chair naturally in a rhythmic patter. The second strongest peak in Figure 14 however is found at 6.6Hz, which is clearly meaningless when compared to the time domain showing the data was taken over a 15 second period. The closest peak of the spectral signal is nearly the strength of the second peak and is found at 1.1Hz, a more realistic and meaningful frequency.

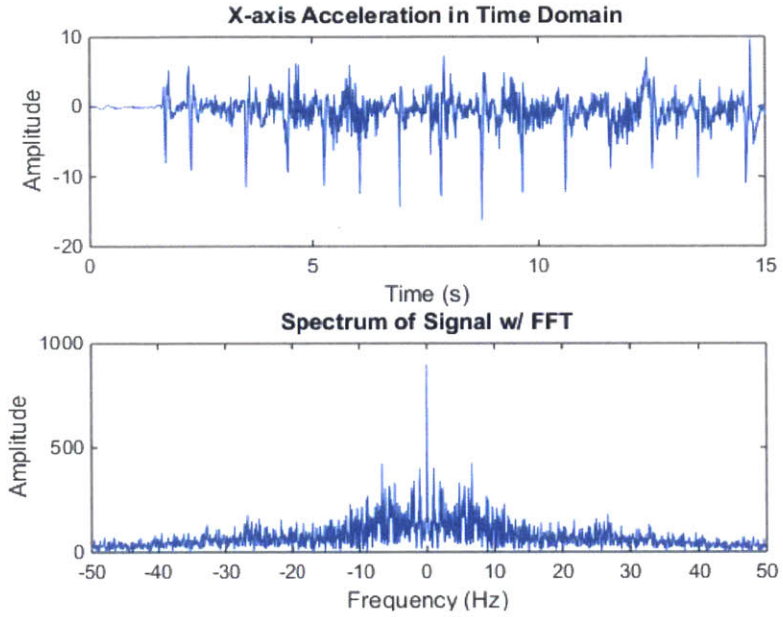

Figure 14: Comparison of the X-axis acceleration data for bumpy terrain in the time and frequency domains.

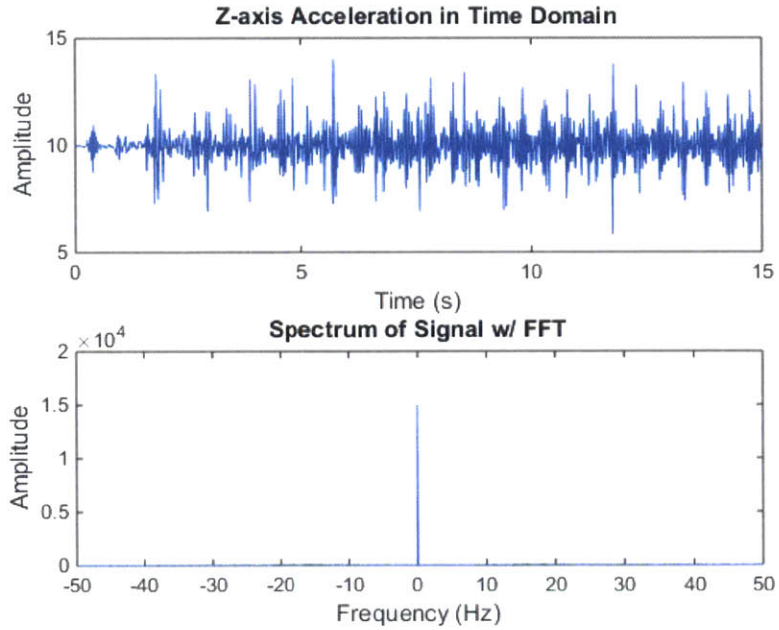

Figure 15: Comparison of the Z-axis acceleration data for flat terrain in the time and frequency domains.

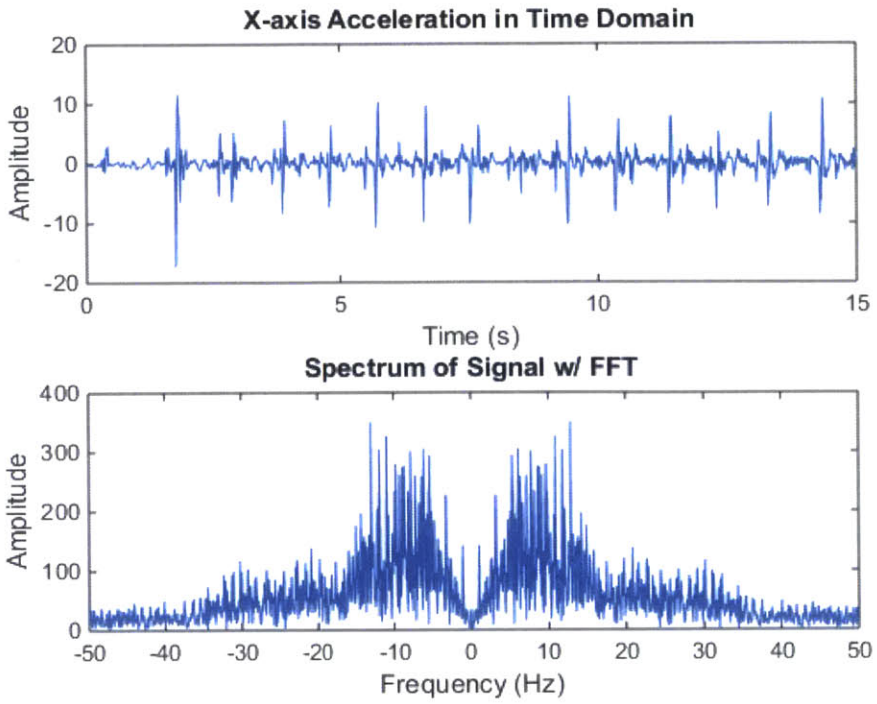

Figure 16: Comparison of the X-axis acceleration data for flat terrain in the time and frequency domains.

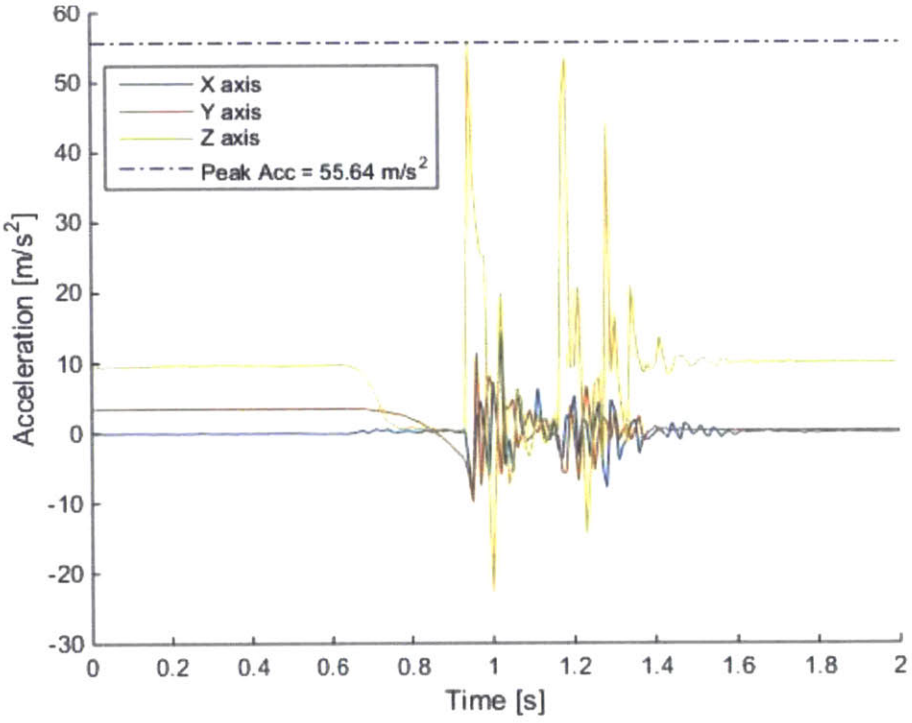

Figure 17: Measured acceleration on the front wheel from a 10 inch drop test.

3.2 Wheel Compression Experimental Design

To determine the stiffness and damping of the original tires and alternatives which could be used as the front wheel of the LFC, multiple samples were tested under compression in an Instron machine. The frame and axle, shown in Figure 18, were fabricated to suspend the wheel in line with the Instron for fixturing such that the application of loading for these experiments would mimic the loading of the wheel when in use as a wheelchair, loaded vertically onto the axle, central hub and bearings.

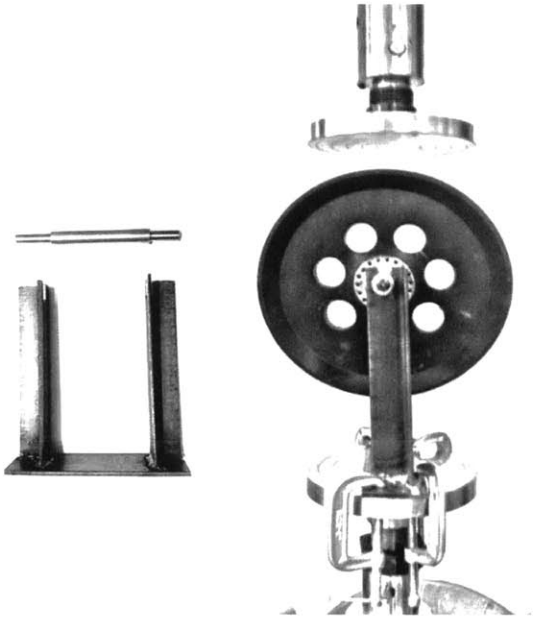

Figure 18: Fabricated fixture and axle for Instron compression testing and when clamped to the Instron.

In conjunction, a flat plate connected to a 10kN load cell was used to apply a 2000N sinuosidal force on the wheel and record the displacement. Testing focused on the effects of a cyclic 2000N load, because it was calculated to be the static loading of the wheel with a safety factor of 2 as explained in section 2.2 Forces. Figure 19 shows the Farm & Ranch FR1055 Pneumatic wheel fixture in the Instron machine and under loading. The Farm & Ranch FR1055 Pneumatic was inflated to 30 psi, the maximum inflation specified for this model. As the other wheels were polyurethane foam or molded rubber no inflation maintenance is necessary.

Figure 19: Fixturing set-up for Instron compression testing of wheel.

During initial setup of the Instron, experimentation and infamiliarity with the machine resulted in a 5,000N force application, upon which the rubber split parralel to the hub as shown in Figure 20. Though 5,000N is above the design criteria it is not an unreasonable amount of force to be incurred on the wheel from high impacts, as will later be seen from the acceleromenter testing data in section 3.1 Original Front Wheel Acceleration Experiment.

Figure 20: Visible crack in rubber of the original wheel caused by a 5,000N compressive load.

This resulting crack was dissimilar to those witnessed in the field. Its placement at the troth of a hole was also not predicted from the SolidWorks SimulationXpress Study, as depicted in Figure 21.

Model name: front wheel
Study name: SimulationXpress Study(-Default-)
Plot type: Factor of Safety Factor of Safety
Criterion : Max von Mises Stress
Red < FOS = 5 < Blue

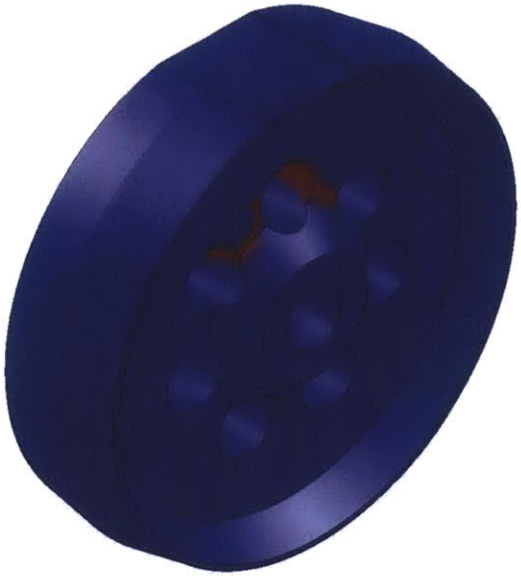

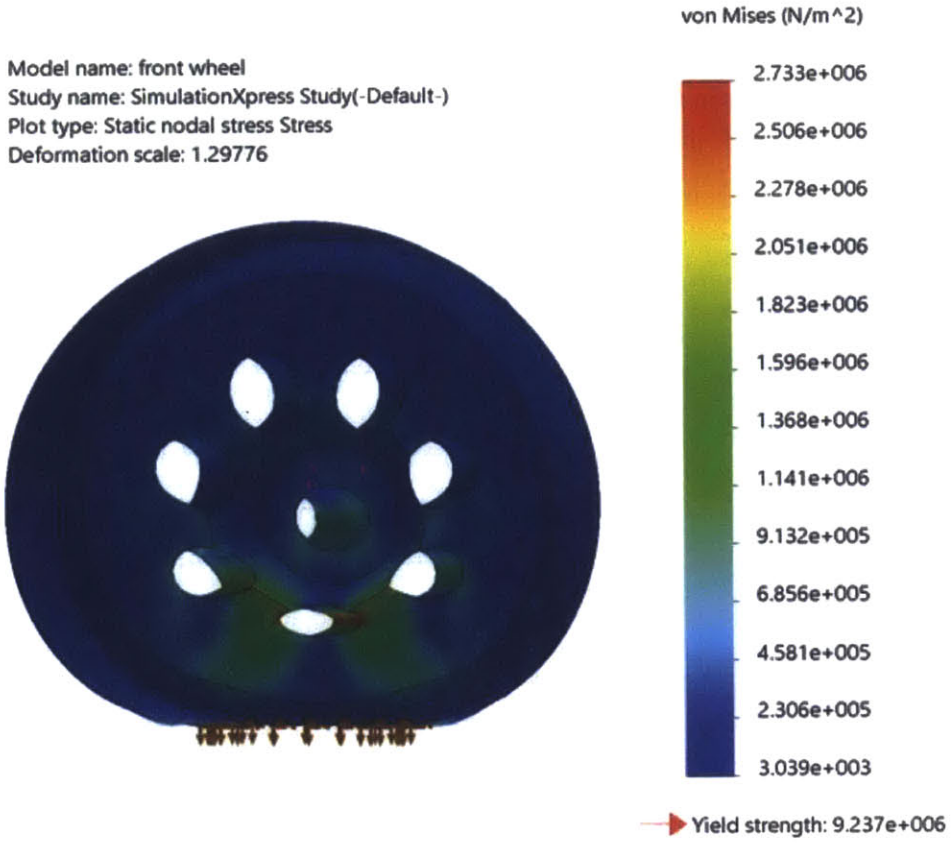

Figure 21: Factor of safety simulation above and Von Mises stress simulation below.

This inconsistency in the model and physical manifestations of the rubber's failure indicated a non-uniformity in the rubber. The delamination of the rubber on the rim of the wheel shown in Figure 6 also falls outside the predicted failure regions, thus supporting the theory of non-uniform, not fully laminated rubber. This error in quality would have been incurred during the wheel molding and manufacturing process.

3.3 Alternative Wheel Selection

A review of wheels which are manufactured for a variety of applications where compared against the functional requirements of the LFC front wheel. Other wheel applications include go-karts, exercise equipment (treadmill), hand trollies, baby strollers, mountain boards, wheel barrows and farm equipment. A predicted desired hardness between Shore A 50-70 was sought, though specifications for wheel hardness were rarely included in the manufacturer's specifications. The wheel geometry was a defining characteristic of the potential for a wheel to be selected for testing, as wheels which would not fit within the existing fork were eliminated from the list of alternatives.

The wheels displayed in Figure 22 were purchased from Amazon for compression and comparison to the original rubber wheel. They were selected for testing based on their consumer availability, approximate size, and intended application on rugged carts and wheel barrows. Two polyurethane foam (PU-foam) sample wheels, the Farm & Ranch FR1030 No-Flat and the Marathon Industries 00210, were of particular interest for there "no-flat" properties, eliminating the need to change a pneumatic tube. More affordable PU-foam wheels were considered, particularly some manufactured by factories which solely produce rubber and PU-foam wheels in China. In bulk purchases the unit price drops dramatically, particularly for the PU-foam wheels which drop in to the range of 2-10USD. The unit prices of each wheel are listed in Table 1.

Figure 22: Top view of wheels which were tested under compression.

The Bugaboo baby stroller wheel is included in the comparison in Table 1 as a precedent from previous work by Ben Judge. However this wheel could not be sourced and failed under minimal loads during preliminary testing so it is not included in the experimental data section.

Wheel	Weight [kg]	Price [USD]	Diameter [in]	Hub Width [mm]
Current Molded India Rubber	1.7	$12	8.75"	100
Bugaboo	0.85	$30	9.75"	53
Farm & Ranch FR1055 Pneumatic	1.6	$13	10"	55
Farm & Ranch FR1030 No-Flat	1.8	$30	10"	55
Mintcraft Cw/w-005p Solid Rubber Hand Truck Wheel	2.9	$13	10"	56
Marathon Industries 00210	1.6	$25	10"	57.15

Table 1: Comparison of wheel characteristics.

The five wheels tested shown from a frontal perspective in Figure 23. The bearing configuration for the two Farm & Ranch and the Marathon Industries wheel are designed for a cantilevered axle configuration, in which a wheel would be attached to either side of a cart so the bearings are offset. As the caster wheel on the front of the LFC utilizes a forked configuration it is important to match that design with a compatible tire on a wheel with a center mounted hub. Very similar alternative wheels that have center mounted hubs are available, though the selection is more limited.

Figure 23: Frontal view of wheels which were tested under compression.

3.4 Compressive Experimental Results and Discussion

The force date shown in Figure 24 verifies the cyclic loading of the Instron machine between 0 and ~2000N at a frequency of 5Hz. A small bit of overshoot is visible due to the PID controller of the Instron machine. The Instron recorded samples with a frequency of 4739 Hz, a data point every 211ms, chosen because it is a prime integer yielding a frequency five times the Nyquist frequency to avoid aliasing.

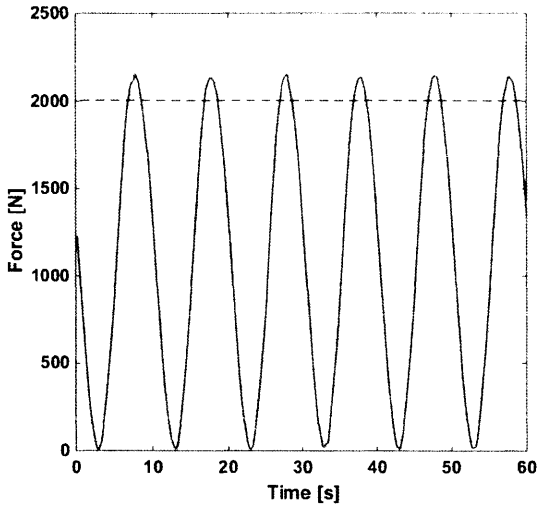

Figure 24: Measured force from the load cell for the original rubber wheel.

Figure 25 depicts the measured data point for each of the five wheels. Red points are distinguished from blue points to show the compressive and decompressive regimes of the loading cycle. Data was taken and accumulated over many cycles. For each cycle the integral within the hysteresis loop was taken, then averaged and compared to determine error ranges. A linear fit was made through the compressive region of the tests to determine a stiffness value [N/m] for each wheel.

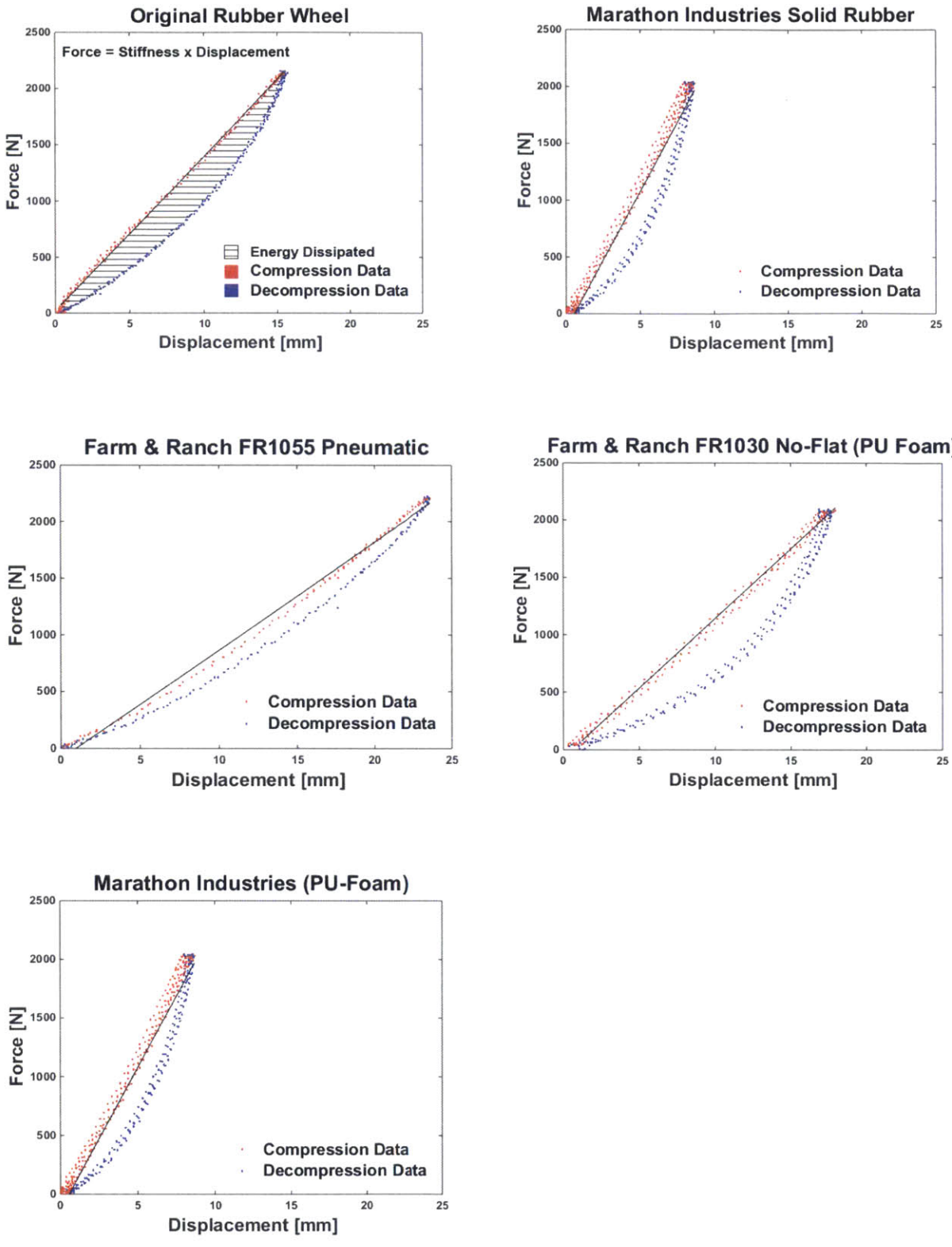

Figure 25: Raw data from Instron showing hysteresis curves for each wheel.

It is interesting to note the consistency of the hysteresis loops through their cycles for the pneumatic and rubber wheels, and the shifting which is visible for the two polyurethane foam wheel tests. Further testing is desired to understand the long term effects of loading, particularly on the two polyurethane foam samples (the Marathon Industries 00210 and the Farm & Ranch FR1030 No-Flat), to understand a time scale and persistence of this shifting on the hysteresis loop. Table 2 shows each of the five wheels tested, a stiffness value, and the average energy dissipated within each wheels hysteresis loop to a 95% confidence level.

Wheel Tested	Stiffness [N/mm]	Energy Dissipated in Hysteresis Curve [J]
Original Molded Rubber	137.5 ± 1.8E-06	29 ± 0.37
Farm & Ranch FR1055 Pneumatic	95.4 ± 1.6E-06	44.1 ± 0.20
Farm & Ranch FR1030 No-Flat (PU Foam)	121.5 ± 1.2E-06	19.2 ± 0.04
Mintcraft Cw/w-005p Solid Rubber	401.7 ± 1.7E-05	9.1 ± 0.33
Marathon Industries 00210 (PU Foam)	249.2 ± 1.4E-06	13.2 ± 0.14

Table 2: Stiffness and energy dissipated in each wheel with 95% confidence.

The data from Table 2 is graphed in Figure 26 to more visually show the results. The Farm & Ranch pneumatic wheel was the most elastic, or least stiff, but it also showed the highest energy absorbed during the testing. There appears to be a rough inverse correlation between stiffness and the amount of energy absorbed.

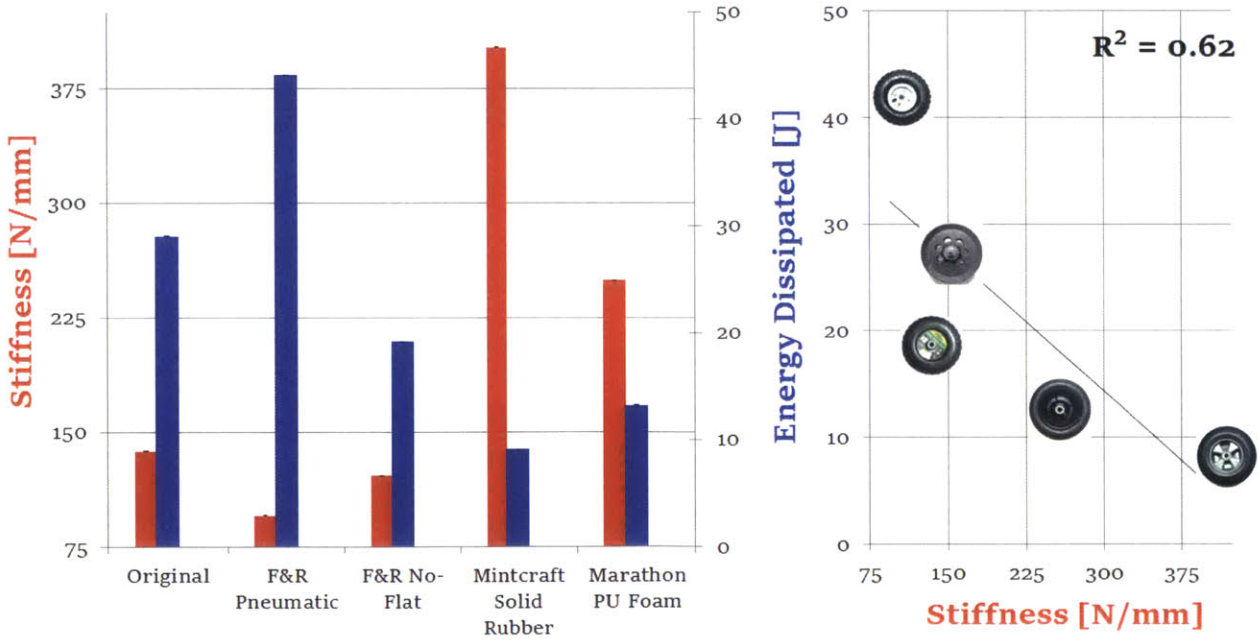

Figure 26: Graphs visually comparing stiffness and energy data for the wheels.

4.0 Dynamic Modeling of the Leveraged Freedom Chair

Using the values determined from the experimental data for the chairs acceleration and the front wheels characteristics a computational, dynamic model of the Leverage Freedom Chair was created. In order to relate the rider's experience to the front wheel, each wheel was modeled as a spring and dashpot in parallel, following the Kelvin-Voigt material model, as shown in Figure 27. The front and the back of the chair where described by a spring constant k and a damping coefficient b. The motion of the chair as it settles from an un-weighted point is described as a function of its angle, θ, and the height at the center of gravity. From the chair's angle and center of gravity height the displacement of each wheel was determined.

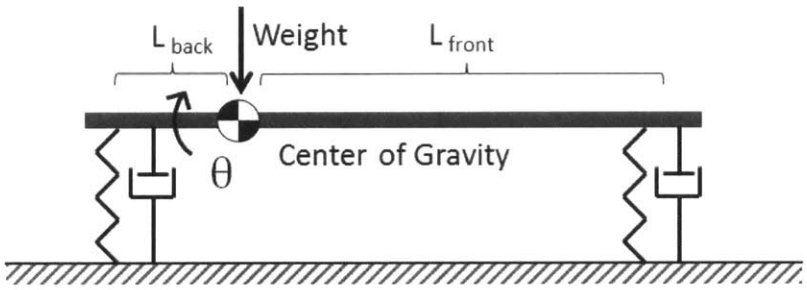

Figure 27: Mechanical model of the LFC replacing the wheels with a spring and dashpot in parallel.

MatLab's ODE45 function was used with the parameters for the front wheels spring constant and damping coefficient from the measured data. Since the back of the chair has two wheels which were not experimented on, it was describes as having twice the spring stiffness and twice the damping as the front wheel. Initial conditions were set to describe the front wheel lifted 10 inches in the air and no loading on the rear two wheels, as the experimental drop was set-up in 3.1 Original Front Wheel Acceleration Experiment. The resulting predictions for the LFC's dynamics are depicted in Figure 28.

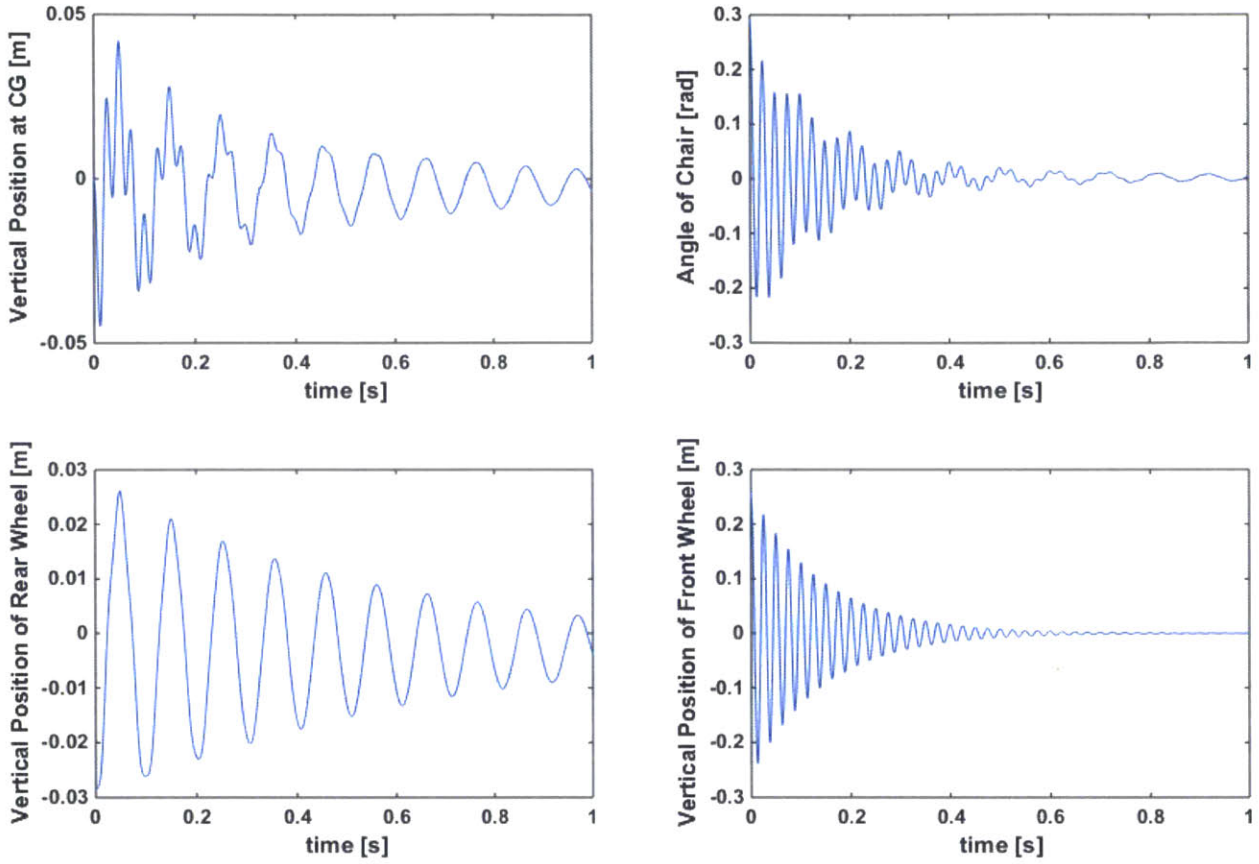

Figure 28: Predicted motion of the LFC resulting from a 10" drop of the front wheel.

Taking the derivative of the predicted vertical height of the front wheel the velocity and acceleration were also determined, and is compared to the measured data in Figure 29. It is seen from this comparison that the computational model could not predict the response with accuracy.

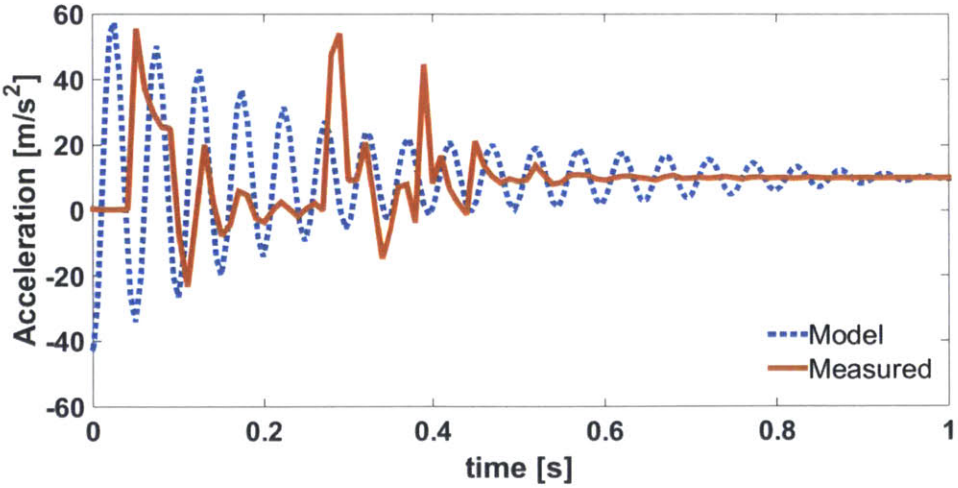

Figure 29: Acceleration on the front wheel as modeled and measured.

5.0 Design Discussion

As the original wheel failed in testing under loads predicted by calculations and experimental measurements, as well as documented failures in the field discontinuation of its use is recommended. An alternative, pre-manufactured wheel is sought which can be purchased. Wheel barrow and hand truck wheels were selected for testing as they are of a similar scale, geometry and also designed for rough terrains and high loads.

The Farm & Ranch FR1055 pneumatic wheel was found to have the least stiffness of the five wheels tested under compression in the Instron machine. This wheel however was also measured to absorb the most energy in a 2,000N cycle at 5Hz. The exact effect of this energy absorption is unknown, but it is expected to have a negative impact on the life span of the wheel and the amount of energy the rider must provide to propel themselves forward. Other considerations for the selection of an alternative wheel however are, in practice, more important than the subtle difference measured between these alternative wheels' stiffness and absorbed energy.

To compare the five wheel alternatives which were tested against the functional requirements, a Pugh chart was constructed to more analytically quantify their differences, show in Table 3. In this chart each wheel alternative was compared against the original rubber wheel and rated as a +, - or 0, for being better, worse, or equal to the original wheel at meeting the specific functional requirement of that column on the chart. As the life span for each wheel was not tested the criteria included a warranty from the manufacturer. If the wheel was rated or warranted for at least a year it received a "+". Weight was an exact, measured comparison. Elasticity was a null, as the wheels elasticity is generally comparable and of order, excluding the Mintcraft Solid Rubber which was dramatically more rigid than the alternatives. For the geometric functional requirement the wheels with "+" earned it for having a larger width than the original wheel, increasing the contact area with the ground and therefore decreasing the pressure. The purchased wheels (excluding the Mintcraft Solid Rubber) also have thread patterns, which is superior to the smooth rubber of the original.

Another functional requirement of the Leveraged Freedom Chair is affordability so people in the developing world who have less disposable income can purchase it. The pricing of the developing world LFC is currently on the order of the next leading competitor, and should not be pushed higher for marketing purposes. The unit cost of the two polyurethane foam wheels exceeded the alternative wheel options, which, when purchased individually, all exceed the unit price of the original rubber wheel. Purchased in bulk however the unit price decreases significantly. Venders also specialize in fabrication of polyurethane foam wheels to this scale and initial discussions with venders in China promise their ability to over-mold the polyurethane foam onto a unique hub, something which is of interest to the GRIT team to keep the cone and bearings center mounted hub configuration for ease of repair.

To compare the price of each wheel they were compared to similar items on Alibaba, a Chinese manufacturing and trading website. As the unit price drops dramatically if the items are purchased in bulk the criteria was that if the unit price on Amazon (where the wheels were purchased for testing) was less than half the price of the Original wheel, it was marked "+".

	Life Span	Weight	Elasticity	Geometry	Price	Total:
Original Rubber	0	0	0	0	0	0
Farm & Ranch Pneumatic	+	+	0	+	+	4
Farm & Ranch No-Flat	+	-	0	+	-	-1
Mintcraft Solid Rubber	0	-	-	-	+	-2
Marathon Industries (PU-foam)	0	+	0	+	0	2

Table 3: Pugh chart comparing wheel alternatives against the functional requirements.

The results of the Pugh chart in Table 3 show the Farm & Ranch Pneumatic wheel as the overall, clear winner, however a main concern for the LFC is the availability of parts. This was not listed in the functional requirements for the wheel as availability is generally a function of price, but for certain items price can vary dramatically depending on location. For the American LFC it is less critical to have locally available components, but for the developing world model it is essential. Users in the developing world do not have access to internet ordering or the ability to easily contact GRIT or distributors for replacements and repairs. Therefore a pneumatic wheel is likely not a good solution for the developing world chair because the availability of replacement tubes would be scarce.

Further work should be conducted into the life span of each wheel, fatigue testing of the tire's material as well as their bearing configuration and performance. Further research should be done to understand the shifting of the hysteresis curve witnessed in the polyurethane foam wheels. However, at this point if the polyurethane foam wheels can be procured at a comparable price as the original wheel it is a promising alternative.

6.0 Conclusion

Based on its performance it is concluded that a pneumatic wheel of comparable geometry to the original rubber wheel is the best alternative for the American chair where maintenance is more routine and replacement parts and service are readily available. For the developing world future work is necessary to either improve the quality of the original rubber wheel or select a low cost, low maintenance alternative. A polyurethane foam wheel, purchased from a factory which specializes in wheel fabrication, looks to be the most promising avenue to meet the functional requirements of the Leveraged Freedom Chair in the developing world.

Bibliography

[1] A. Winter, M. Bollini, D. DeLatte, B. Judge, H. O'Hanley, J. Peralman, and N. Scolnik, "The Design, Fabrication, and Performance of the East African Trial Leveraged Freedom Chair," presented at the ASME 2010 International Design Engineering Technical Conference & Computers and Information in Engineering Conference, Montreal, Quebec, Canada, 2010.

[2] J. A. Sherwood, "Constitutive Modeling and Simulation of Energy Absorbing Polyurethane Foam Under Impact Loading," *Polymer Engineering and Science*, no. Vol. 32, No. 16, Aug. 1992.

[3] "GRIT Leveraged Freedom Chair." [Online]. Available: http://gogrit.org/lfc.html. [Accessed: 06-Apr-2015].

[4] L. Anand, "Introduction to the Mechanical Behavior of Materials," 31-Jan-2011.

[5] L. J. Gibson and M. F. Ashby, *Cellular Solids: Structure & Properties*. Pergamon Press, 1988.

[6] M. Bolinni and B. Judge, "LFC Front Wheel Thesis," 14-Feb-2015.

[7] "Motivation | Wheelchairs." [Online]. Available: http://www.motivation.org.uk/our-products/wheelchairs/. [Accessed: 08-May-2015].

[8] R. C. Hibbeler, *Mechanics and Materials*, Eighth. USA: Prentice Hall.

[9] J. M. Walton, "The Design of a Frame for an All Terrain, Lever Propelled Wheelchair," Massachusetts Institute of Technology, 2011.

[10] B. Judge, "The Research and Design of a Low Cost, All Terrain, Mechanically Advantageous Wheelchair for Developed Markets," Massachusetts Institute of Technology, 2011.

[11] G. J. Lake and A. G. Thomas, "The Strength of Highly Elastic Materials," *Proceedings of the Royal Society of London A: Mathematical, Physical and Engineering Sciences*, vol. 300, no. 1460, pp. 108–119, Aug. 1967.

[12] S. Ahuja, "Wheel Vulcanization Process," 09-Mar-2015.

[13] Williams, *Fundamentals of Applied Dynamics*. John Wiley & Sons, Inc., 1996.